

Holographic dark energy in Rastall theory

S. Ghaffari^{1*}, A. A. Mamon^{2†}, H. Moradpour^{1‡}, A. H. Ziaie^{1§}

¹ *Research Institute for Astronomy and Astrophysics of Maragha (RIAAM),
University of Maragheh, P.O. Box 55136-553, Maragheh, Iran*

² *Department of Physics, Vivekananda Satavarshiki Mahavidyalaya (affiliated
to the Vidyasagar University), Manikpara-721513, West Bengal, India*

Bearing holographic dark energy hypothesis in mind, the ability of vacuum energy in describing the current accelerated universe is studied in the framework of Rastall theory. Here, in addition to the ordinary approach in which it is expected that this energy plays the role of dark energy, we also address a new approach where the sum of this energy and Rastall term is responsible for the current accelerated universe. We also investigate the cosmological outcomes of using Tsallis entropy in quantifying the energy of fields in vacuum for both mentioned approaches. The implications of considering an interaction between the various segments of cosmic fluid have been addressed in each studied cases. The normalized Hubble parameter for the models have also been plotted and compared that with the $H(z)$ data consisting of 41 data points in the redshift range of $0.07 \leq z \leq 2.36$.

I. INTRODUCTION

Motivated by the long-range nature of gravity, the use of generalized entropies to study Cosmos has recently been proposed [1–4]. In this regard, it has been shown that the Tsallis entropy can make a bridge between Verlinde and Padmanabhan hypothesis, and additionally, be combined with thermodynamic laws to modify Friedmann equations in a way that the outcomes can explain the accelerated universe without considering a mysterious dark energy source [1]. In this regard, relying on the holographic dark energy hypothesis [5–11], and using Tsallis entropy, a new holographic dark energy, namely Tsallis holographic dark energy model (THDE), is also introduced in Ref. [12].

In the Einstein framework, where the horizon entropy meets the Bekenstein entropy, while there is not any mutual interaction between the Cosmos sectors, both HDE models, obtained by taking into account the radius of apparent horizon as the IR cutoff, and pressureless source are scaled with the same function of Hubble parameter [9]. This difficulty may be solved by using generalized entropy based on HDE models such as THDE [12]. There are observational and theoretical works admitting the breakdown of the conservation law (the backbone of general relativity) in curved spacetime [4, 13–15], a point which has firstly been noted by P. Rastall [16].

Although, Rastall gravity produces acceptable and suitable predictions and explanations for various gravitational and cosmological phenomena [15, 17–20], it is shown that a dark energy-like source is still needed to describe the current accelerated universe in this framework, if we assume that the universe is filled by cosmic

fluids with constant equation of state [21, 22]. A recent study addresses its conflicts and agreements with observations by considering a universe in which a constant plays the role of vacuum energy (as the dark energy candidate) and other cosmic fluids have constant equation of state (Rastall- Λ CDM model) [23]. Their study also focus on linear perturbations, while it seems that non-linear perturbations reveal differences between the Rastall cosmology and the Λ CDM model [22], and it finally signals us that *i*) more observations may be needed to decide about allowed values of the parameter of Rastall theory, and *ii*) a general form of this theory may solve confusion in the current value of Hubble parameter [23].

In fact, using the holographic hypothesis, one can get an estimation for the vacuum energy helping us in studying its cosmological consequences [5]. In the next section, we are going to study the cosmological implications of vacuum energy in the Rastall framework by employing the holographic hypothesis, and using horizon entropy obtained by applying the thermodynamic laws to horizon in Rastall theory [17, 18]. In Sec. (III), applying Tsallis entropy to horizon, we shall investigate the ability of modelling dark energy by using THDE in the Rastall framework. In each cases, the effects of considering a mutual interaction between dark energy candidate and other segments of cosmos are also studied. Moreover, we also propose a new candidate for dark energy i.e., the sum of vacuum energy and Rastall term. The ability of considering this hypothesis in describing the current Cosmos has also been studied in Secs. (II) and (III). The observational constraints are also addressed throughout the paper. The last section includes the summary of work, and the units have been set so that $c = \hbar = k_B = 1$.

II. HDE IN RASTALL THEORY

Since the WMAP data indicates a flat universe [24], here, we only focus on flat FRW universe with line element

*sh.ghaffari@riaam.ac.ir

†abdulla.physics@gmail.com

‡hn.moradpour@maragheh.ac.ir

§ah.ziaie@maragheh.ac.ir

$$ds^2 = -dt^2 + a(t)^2[dr^2 + r^2(d\theta^2 + \sin(\theta)^2 d\phi^2)], \quad (1)$$

in which $a(t)$ is called the scale factor. The apparent horizon of this spacetime, as a proper casual boundary, is also located at [4, 17, 18]

$$\tilde{r}_A = \frac{1}{H}, \quad (2)$$

and hence, $A = \frac{4\pi}{H^2}$ is the horizon area. The Rastall field equations are written as [16]

$$G_{\mu\nu} + \kappa\lambda g_{\mu\nu}R = \kappa T_{\mu\nu}, \quad (3)$$

leading to

$$(12\kappa\lambda - 3)H^2 + 6\kappa\lambda\dot{H} = -\kappa\rho, \quad (4)$$

and

$$(12\kappa\lambda - 3)H^2 + (6\kappa\lambda - 2)\dot{H} = \kappa p, \quad (5)$$

as the corresponding Friedmann equations. In the above equations, λ and k denote the Rastall parameter and the Rastall gravitational coupling, respectively. Considering the Newtonian limit, one can obtain [16, 17]

$$\kappa = \frac{4\eta - 1}{6\eta - 1}\kappa_G, \quad \lambda = \frac{\eta(6\eta - 1)}{(4\eta - 1)\kappa_G}, \quad (6)$$

in which $\kappa_G = 8\pi G$ is the Einstein gravitational coupling and $\eta = \kappa\lambda$. Continuity equation governing the cosmic fluid with energy density ρ and pressure p is [4, 18]

$$\left(\frac{3\eta - 1}{4\eta - 1}\right)\dot{\rho} + \left(\frac{3\eta}{4\eta - 1}\right)\dot{p} + 3H(\rho + p) = 0. \quad (7)$$

If the Cosmos is filled by a pressureless source with energy density ρ_m and another fluid with energy density ρ_Λ and pressure p_Λ , then the Friedmann equations take the form

$$(12\eta - 3)H^2 + 6\eta\dot{H} = \frac{4\eta - 1}{1 - 6\eta}\kappa_G(\rho_\Lambda + \rho_m),$$

$$(12\eta - 3)H^2 + (6\eta - 2)\dot{H} = \frac{4\eta - 1}{6\eta - 1}\kappa_G p_\Lambda, \quad (8)$$

leading to

$$\dot{H} = \frac{4\eta - 1}{2(1 - 6\eta)}\kappa_G(\rho_\Lambda + \rho_m + p_\Lambda). \quad (9)$$

Whenever there is not any mutual interaction between both dark components. Eq. (7) is decomposed to

$$\left(\frac{3\eta - 1}{4\eta - 1}\right)\dot{\rho}_m + 3H\rho_m = 0 \rightarrow \rho_m = \rho_0 a^{\frac{3(1-4\eta)}{3\eta-1}}, \quad (10)$$

where ρ_0 is the integration constant, and

$$\left(\frac{3\eta - 1}{4\eta - 1}\right)\dot{\rho}_\Lambda + \left(\frac{3\eta}{4\eta - 1}\right)\dot{p}_\Lambda + 3H(\rho_\Lambda + p_\Lambda) = 0. \quad (11)$$

Since, in the Rastall framework, we have $S = \left(\frac{6\eta-1}{4\eta-1}\right)\frac{A}{4G}$ for the horizon entropy [17, 18], by following the original HDE hypothesis [5], one easily reaches

$$\rho_\Lambda = \frac{3B}{8\pi G}\left(\frac{6\eta - 1}{4\eta - 1}\right)H^2, \quad (12)$$

where B is a numerical constant as usual. Inserting this result in the first line of Eq. (8), we can check that $\rho_m \approx \frac{H^2}{\rho_\Lambda}$ whenever $\eta = 0$ or even whenever $\eta \neq 0$ and $w_\Lambda \equiv \frac{p_\Lambda}{\rho_\Lambda} = \text{constant}$. Therefore, the same as the Einstein framework ($\eta = 0$) [9], dark energy and ρ_m will be scaled by the same function of H in the Rastall framework if $\eta \neq 0$ and $w_\Lambda = \text{constant}$. It means that we should have $w_\Lambda \neq \text{constant}$ to avoid this difficulty in the Rastall framework.

A. Common approach

From Eq. (8), by defining critical density ρ_c as $\rho_c \equiv \frac{3H^2}{8\pi G}$, we get

$$1 = \frac{4\eta - 1}{6\eta - 1}(\Omega_m + \Omega_\Lambda) + \Omega_\eta + 4\eta, \quad (13)$$

in which

$$\Omega_m = \frac{\rho_m}{\rho_c}, \quad \rho_\eta \equiv \frac{6\eta\dot{H}}{8\pi G}, \quad (14)$$

$$\Omega_\eta = \frac{\rho_\eta}{\rho_c} = \frac{2\eta\dot{H}}{H^2}, \quad \Omega_\Lambda = \frac{\rho_\Lambda}{\rho_c} = B\frac{6\eta - 1}{4\eta - 1}.$$

Now, using Eqs. (8), (14) and (12), one can obtain the EoS and deceleration parameters as

$$\omega_\Lambda = \frac{1}{B}\left(\frac{\Omega_\eta(3\eta - 1)}{3\eta} + 4\eta - 1\right), \quad (15)$$

and

$$q = -1 - \frac{\dot{H}}{H^2} = -1 - \frac{\Omega_\eta}{2\eta}, \quad (16)$$

respectively, which are, in effect, the same for both non-interacting and interacting cases. At the classical level,

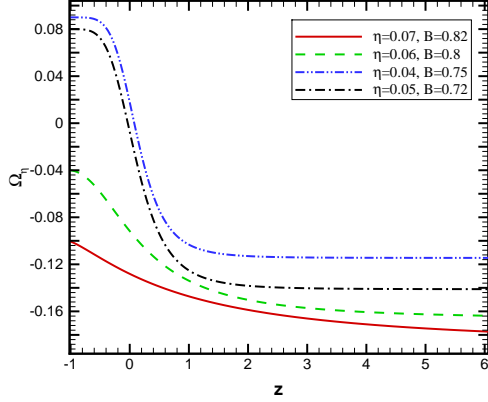


FIG. 1: Ω_η versus z for non-interacting HDE in Rastall theory for some values of η and B .

the stability of an energy source with energy density ρ and pressure p is also determined by the sign of the sound speed square (v_s^2) evaluated as

$$v_s^2 = \frac{dp_\Lambda}{d\rho_\Lambda} = \frac{\dot{p}_\Lambda}{\dot{\rho}_\Lambda} = w_\Lambda + \frac{\dot{w}_\Lambda \rho_\Lambda}{\dot{\rho}_\Lambda}. \quad (17)$$

In the following, we study the HDE model in the Rastall theory for both non-interacting and interacting cases .

Non-interacting Case

Taking the time derivative of the first Friedmann Eq. (8), and combining the result with Eqs. (10), (11), (12) and (14), one finds

$$\frac{\ddot{H}}{H^3} = \frac{4\eta - 1}{2\eta(1 - 6\eta)} \left[\frac{3\Omega_\eta(6\eta - 1)}{3\eta - 1} + (\Omega_\Lambda + 6\eta - 1) \left(\frac{\Omega_\eta}{\eta} + \frac{3(4\eta - 1)}{3\eta - 1} \right) \right], \quad (18)$$

which can be used to write

$$\Omega'_\eta = \frac{\dot{\Omega}_\eta}{H} = \frac{4\eta - 1}{1 - 6\eta} \left[\frac{3\Omega_\eta(6\eta - 1)}{3\eta - 1} + (\Omega_\Lambda + 6\eta - 1) \left(\frac{\Omega_\eta}{\eta} + \frac{3(4\eta - 1)}{3\eta - 1} \right) \right] - \frac{\Omega_\eta^2}{\eta}, \quad (19)$$

where prime denotes derivative with respect to $x = \ln a$, and we used $\dot{\Omega}_\eta = H\Omega'_\eta$. We have plotted the evolution of Ω_η versus redshift parameter z in Fig. 1 for some values of η and B . The behavior of ω_Λ and q are also plotted in Fig. 2. As it is obvious, Universe has a transition from a deceleration phase to the current accelerated phase at

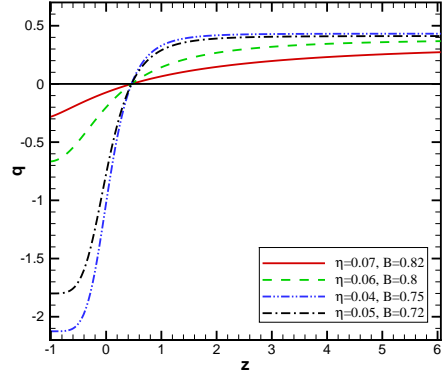
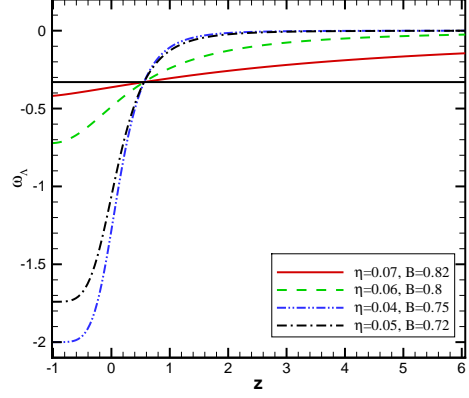


FIG. 2: The evolution of the equation of state and deceleration parameters with respect to the redshift for non-interacting HDE in Rastall theory.

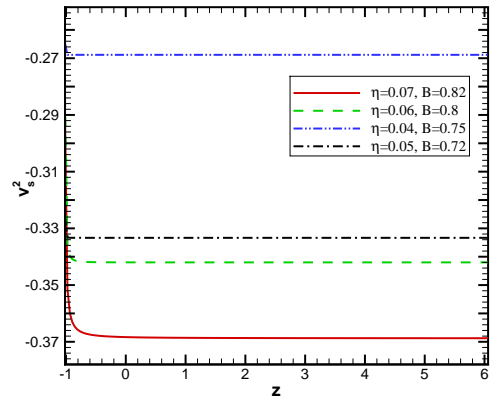


FIG. 3: v_s^2 versus z for non-interacting HDE in Rastall theory for some values of η and B .

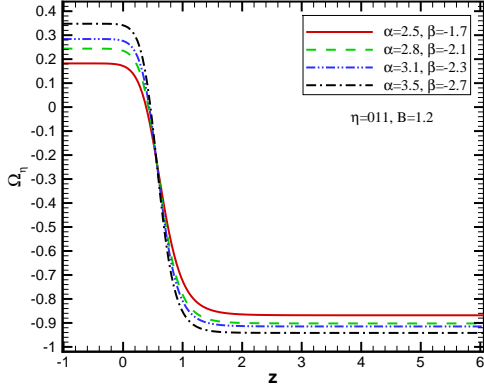


FIG. 4: Ω_η versus z for interacting HDE in Rastall theory. we have taken $\eta = 0.11$ and some values of B , α and β .

the redshift $z \approx 0.6$ in agreement with the recent observation data [26], and the EoS parameter can not cross the phantom line. For studying the classical stability of the dark energy model (ρ_Λ), by taking the time derivative of Eq. (15) and employing Eqs. (12) and (19), we reach

$$v_s^2 = \frac{4\eta - 1}{B} + \frac{4\eta - 1}{3B\eta(1 - 6\eta)\Omega_\eta} \left(3\eta(6\eta - 1)\Omega_\eta + (\Omega_\Lambda + 6\eta - 1)(3\eta(4\eta - 1) + (3\eta - 1)\Omega_\eta) \right), \quad (20)$$

plotted in Fig. 3 versus redshift parameter. We see that the square of sound speed is always negative during the evolution of Universe meaning that the non-interacting HDE in Rastall theory is classically unstable, a behavior obtained in the framework of standard cosmology in which HDE plays the role of dark energy [10].

An interacting Case

In the presence of mutual interaction between DM and HDE, the conservation equations are given as [25–28]

$$\begin{aligned} \left(\frac{3\eta - 1}{4\eta - 1}\right)\dot{\rho}_m + 3H\rho_m &= Q, \\ \left(\frac{3\eta - 1}{4\eta - 1}\right)\dot{\rho}_\Lambda + \left(\frac{3\eta}{4\eta - 1}\right)\dot{p}_\Lambda + 3H(\rho_\Lambda + p_\Lambda) &= -Q, \end{aligned} \quad (21)$$

where Q denotes the interaction term and we assume that it has the form $Q = H(\alpha\rho_m + \beta\rho_D)$, in which α and β are unknown coupling constants [25]. Using Eqs. (12), (21), and the time derivative of Eq. (8), we reach

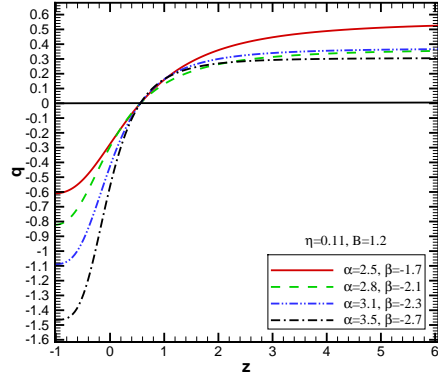
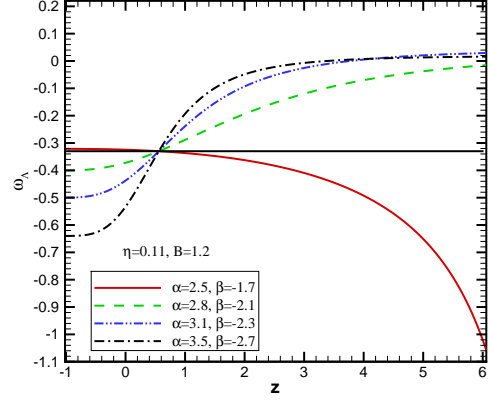


FIG. 5: The evolution of ω_Λ and q with respect to z for interacting HDE in Rastall theory.

$$\begin{aligned} \frac{\ddot{H}}{H^3} &= \frac{4\eta - 1}{2\eta(1 - 6\eta)} \left[\frac{\Omega_\eta(\alpha - 3)(6\eta - 1)}{1 - 3\eta} \right. \\ &+ (\Omega_\Lambda + 6\eta - 1) \left(\frac{\Omega_\eta}{\eta} + \frac{(\alpha - 3)(4\eta - 1)}{1 - 3\eta} \right) \\ &\left. + \frac{(4\eta - 1)\beta\Omega_\Lambda}{3\eta - 1} \right], \end{aligned} \quad (22)$$

used in order to write

$$\begin{aligned} \Omega'_\eta &= \frac{4\eta - 1}{(1 - 6\eta)} \left[\frac{\Omega_\eta(\alpha - 3)(6\eta - 1)}{1 - 3\eta} \right. \\ &+ (\Omega_\Lambda + 6\eta - 1) \left(\frac{\Omega_\eta}{\eta} + \frac{(\alpha - 3)(4\eta - 1)}{1 - 3\eta} \right) \\ &\left. + \frac{(4\eta - 1)\beta\Omega_\Lambda}{3\eta - 1} \right] - \frac{\Omega_\eta^2}{\eta}. \end{aligned} \quad (23)$$

The evolution of Ω_η against redshift z has been plotted in Fig. 4 for the initial condition $\Omega_\Lambda(z = 0) = 0.73$.

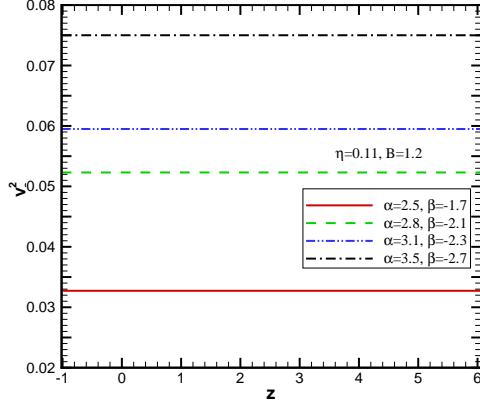


FIG. 6: v_s^2 versus z for interacting HDE in Rastall theory for $\eta = 0.11$ and some values of B , α and β .

We have also plotted the evolution of the EoS and deceleration parameters against redshift z for some values of parameters in Fig. 5. From this figure, one can clearly see the transition redshift z_t lies within the interval $0.5 < z < 0.8$.

By taking the time derivative of Eq. (15) and combining the result with Eqs. (12) and (23), we reach at

$$v_s^2 = \frac{4\eta - 1}{B} + \frac{4\eta - 1}{3B(1 - 6\eta)\Omega_\eta} \left[(3 - \alpha)(6\eta - 1)\Omega_\eta + (\Omega_\Lambda + 6\eta - 1) \left((3 - \alpha)(4\eta - 1) + \frac{(3\eta - 1)\Omega_\eta}{\eta} \right) + (4\eta - 1)\beta\Omega_\Lambda \right]. \quad (24)$$

The evolution of v_s^2 versus redshift parameter is plotted in Fig. 6 showing that the interacting HDE model in Rastall theory, unlike the non-interacting case, is classically stable.

B. A new approach

Here, we assume DE is a combination of the Rastall term and vacuum energy. In this case, Eqs. (8) can be rewritten as

$$3H^2 = \kappa(\rho_m + \rho_D), \quad (25)$$

$$H^2 + \frac{2}{3}\dot{H} = -\frac{\kappa}{3}p_D,$$

where

$$\rho_D = \rho_\Lambda + \frac{6\eta(6\eta - 1)}{\kappa_G(4\eta - 1)}(2H^2 + \dot{H}),$$

$$p_D = p_\Lambda - \frac{6\eta(6\eta - 1)}{\kappa_G(4\eta - 1)}(2H^2 + \dot{H}). \quad (26)$$

It is easy to see that the standard cosmology is restored at the appropriate limit $\eta \rightarrow 0$. Indeed, we wrote the Friedmann equations in a form easily comparable with the standard Friedmann equations. In this case, by defining critical density as $\rho_c = \frac{3H^2(6\eta - 1)}{\kappa_G(4\eta - 1)}$, and using Eq. (25), one can find

$$\Omega_m + \Omega_D = 1, \quad (27)$$

where

$$\Omega_m = \frac{\rho_m}{\rho_c} = \frac{\kappa\rho_m}{3H^2}, \quad \Omega_\Lambda = \frac{\rho_\Lambda}{\rho_c} = B$$

$$\Omega_D = \Omega_\Lambda + 4\eta + 2\eta\frac{\dot{H}}{H^2}. \quad (28)$$

The use of Eq. (25) leads also to

$$\omega_D = \frac{-1}{\Omega_D} \left(1 + \frac{2\dot{H}}{3H^2} \right). \quad (29)$$

Taking the time derivative of Eq. (28), we obtain

$$\dot{\Omega}_D = 2\eta \left(\frac{\ddot{H}}{H^2} - 2\frac{\dot{H}^2}{H^3} \right). \quad (30)$$

For the limiting case $\eta \rightarrow 0$, the equation of motion of HDE in standard cosmology ($\Omega_D = \Omega_\Lambda = const$), as a desired result, is restored.

Substituting Eq. (28) into (29), one can obtain the EoS as

$$\omega_D = \frac{-1}{3\eta\Omega_D} (\Omega_D - \Omega_\Lambda - \eta). \quad (31)$$

Using Eq. (28), one also finds

$$q = -1 - \frac{\dot{H}}{H^2} = \frac{-1}{2\eta} (\Omega_D - \Omega_\Lambda - 2\eta). \quad (32)$$

Hence, it is obvious that at $\eta \rightarrow 0$ ($\Omega_D = \Omega_\Lambda$) limit, the EoS and deceleration parameters for the HDE in standard cosmology are recovered. It is also useful to mention that Eq. (31) and (32) are the same for both non-interacting and interacting cases.

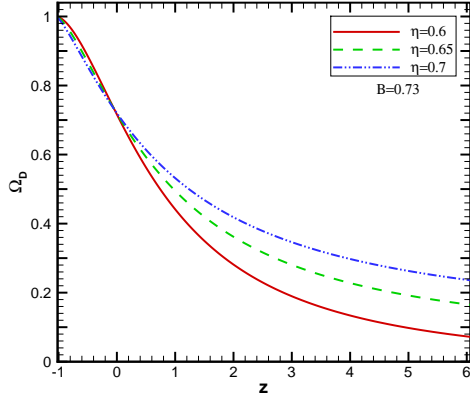


FIG. 7: Ω_D versus z for non-interacting HDE model for $\Omega_D(z=0) = 0.73$, $B = 0.73$ and some values of η .

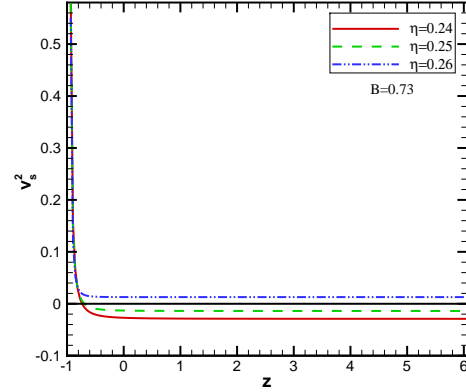


FIG. 9: $v_s^2(z)$ for non-interacting HDE for some values of α and β .

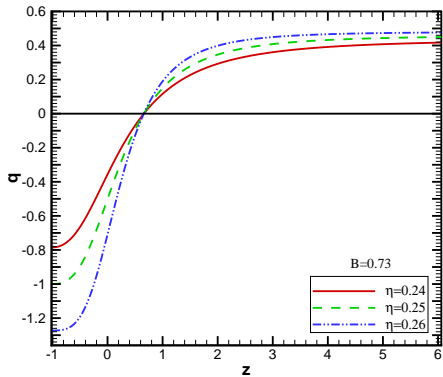
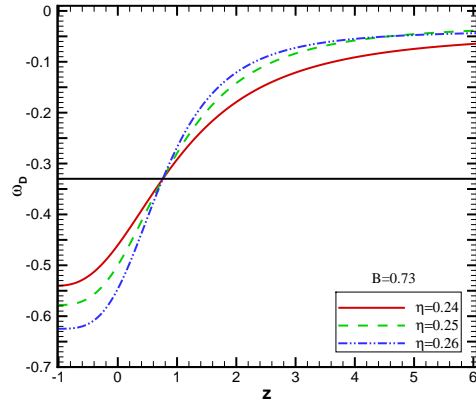


FIG. 8: The evolution of ω_D and q versus z for the non-interacting HDE in Rastall theory for $B = 0.73$ and some values of η .

Non-interacting Case

Combining Eqs. (10), (12), (27) and (28) with the time derivative of the first Friedmann equation (25), we arrive

$$\frac{\ddot{H}}{H^3} = \frac{3(4\eta - 1)(\Omega_D - 1)}{2\eta(1 - 3\eta)} - \frac{1}{2\eta^2}(\Omega_\Lambda + 4\eta - 1)(\Omega_D - \Omega_\Lambda - 4\eta). \quad (33)$$

Inserting Eqs. (28) and (33) into (30), we can also obtain the evolution of dimensionless DE density parameter as

$$\Omega'_D = (\Omega_D - 1) \left(\frac{3(4\eta - 1)}{1 - 3\eta} - \frac{\Omega_D - \Omega_\Lambda - 4\eta}{\eta} \right). \quad (34)$$

The evolution of Ω_D against redshift z has been plotted in Fig.7 for the initial condition $\Omega_D(z=0) = 0.73$ and some values of η , addressing us that $\Omega_D \rightarrow 0$ and $\Omega_D \rightarrow 1$ at the early time and late time, respectively. Moreover, the behavior of $\omega_D(z)$ and $q(z)$ are shown numerically in Fig. 8 for some values of the parameter η which implies that Universe has experienced a transition at the redshift $z \approx 0.6$, and the EoS parameter can not cross the phantom divide ($\omega_D = -1$). Combining Eqs. (12), (37), (36), and the time derivative of Eq. (31) with Eq. (17), we get

$$v_s^2 = \frac{dp_D}{d\rho_D} = \frac{-1}{3\eta\Omega_D} \left(\Omega_D - \Omega_\Lambda - \eta \right) - \frac{(\Omega_\Lambda + \eta)(1 - \Omega_D)}{3\Omega_D} \left(\frac{3(4\eta - 1)}{1 - 3\eta} - \frac{\Omega_D - \Omega_\Lambda - 4\eta}{\eta} \right) \times \left(\frac{1 - 3\eta}{3\eta(4\eta - 1)(\Omega_D - 1) + (1 - 3\eta)(\Omega_D - \Omega_\Lambda - 4\eta)} \right), \quad (35)$$

plotted in Fig. 9 for non-interacting case. It is therefore seen that the stability of this case depends on the value

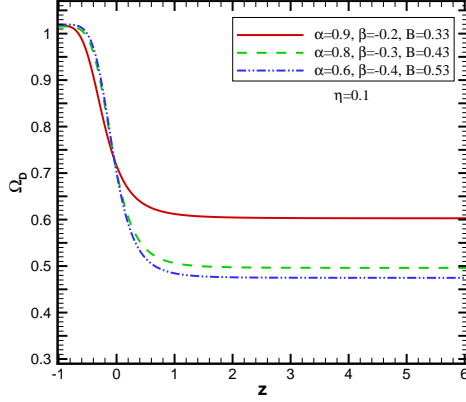


FIG. 10: Ω_D versus z for interacting HDE for some values of B , α and β .

of Rastall parameter so that there exists a critical value for this parameter that lies within the interval $0.25 < \eta_c < 0.26$ and separates the stable and unstable regimes. Therefore we have classical stability (un-stability) for $\eta > \eta_c$ ($\eta < \eta_c$).

An interacting Case

Taking the time derivative of Eq.(25) along with using Eqs. (12), (21), (27) and (28), we reach at

$$\begin{aligned} \frac{\ddot{H}}{H^3} &= \frac{4\eta - 1}{2\eta(1 - 3\eta)}((\alpha - 3)(1 - \Omega_D) + \beta\Omega_\Lambda) \\ &- \frac{1}{2\eta^2}(\Omega_\Lambda + 4\eta - 1)(\Omega_D - \Omega_\Lambda - 4\eta). \end{aligned} \quad (36)$$

Inserting Eq. (36) into (30), one gets

$$\begin{aligned} \Omega'_D &= \frac{4\eta - 1}{1 - 3\eta}((\alpha - 3)(1 - \Omega_D) + \beta\Omega_\Lambda) \\ &- \frac{1}{\eta}(\Omega_D - 1)(\Omega_D - \Omega_\Lambda - 4\eta), \end{aligned} \quad (37)$$

plotted as a function of z in Fig. 10 for the initial condition $\Omega_D(z = 0) = 0.73$. In this manner, while we have $\Omega_D \rightarrow 1$ at the late time ($z \rightarrow -1$), $0.2 < \Omega_D < 0.3$ at the early time ($z \rightarrow \infty$), in agreement with Eq. (28) where the DE density parameter is a combination of the Rastall term and vacuum energy.

Figure. 11 includes the evolution of $\omega_D(z)$ and $q(z)$ for some values of α and β parameters, and indicates that there is a transition from the deceleration phase to the accelerated phase in the interval $0.5 < z_t < 0.9$. It is also seen that, in this case, the interacting HDE model behaves like the phantom DE at the late time.

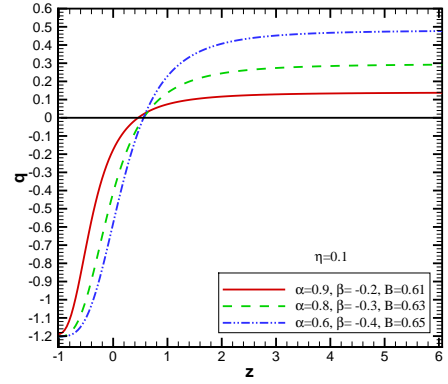
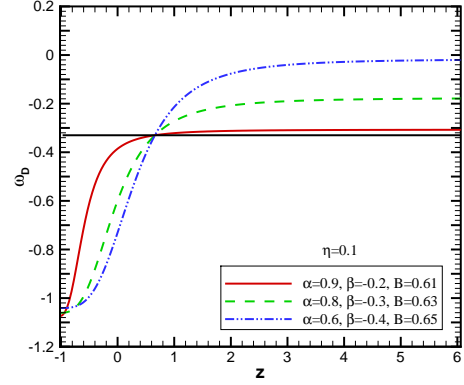


FIG. 11: The evolution of the ω_D and q parameters with respect to the z for interacting HDE in Rastall theory.

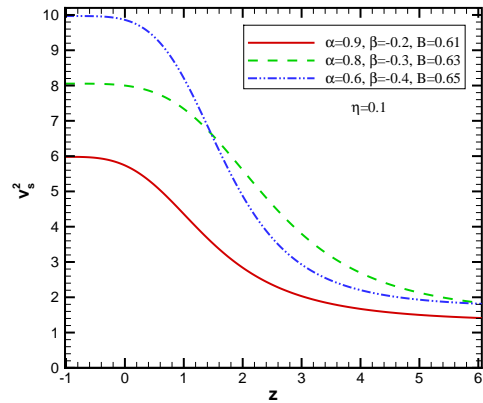


FIG. 12: $v_s^2(z)$ for the interacting HDE for some values of B , α and β .

III. THDE IN RASTALL GRAVITY

Following [12], THDE density in Rastall theory is obtained as

$$\rho_T = \frac{3B}{8\pi G} \left(\frac{6\eta - 1}{4\eta - 1} \right) H^{4-2\delta}, \quad (38)$$

where δ and B are unknown parameters.

A. The common approach

Using definition (14), we can write THDE dimensionless density parameter and its evolution as

$$\Omega_T = B \left(\frac{6\eta - 1}{4\eta - 1} \right) H^{2-2\delta}, \quad (39)$$

and

$$\Omega'_T = \frac{(1 - \delta)\Omega_T\Omega_\eta}{\eta}, \quad (40)$$

respectively. One can also use Eqs. (8), (14) and (38) in order to obtain EoS and deceleration parameters as

$$\omega_T = \frac{(4\eta - 1)\Omega_T}{B^2(6\eta - 1)} \left(\frac{(3\eta - 1)\Omega_\eta}{\eta} + 4\eta - 1 \right), \quad (41)$$

and

$$q = -1 - \frac{\Omega_\eta}{2\eta}, \quad (42)$$

respectively, which are, indeed, the same for both non-interacting and interacting cases.

Non-interacting case

Taking the time derivative of the first Friedmann equation. (8), and putting Eqs. (10), (14), (38) and (39) in the result, we reach at

$$\begin{aligned} \Omega'_\eta &= \frac{3(4\eta - 1)\Omega_\eta}{1 - 3\eta} - \frac{\Omega_\eta^2}{\eta} \\ &+ \frac{4\eta - 1}{\eta(1 - 6\eta)} \left[\frac{3\eta(4\eta - 1)}{3\eta - 1} (\Omega_T + 6\eta - 1) \right. \\ &\left. + ((2 - \delta)\Omega_T + 6\eta - 1)\Omega_\eta \right]. \end{aligned} \quad (43)$$

Ω_T , ω_T and q versus the redshift parameter z have been plotted in Figs. 13 and 14 for non-interacting THDE in common approach. Although $\Omega_T(z)$, $\omega_T(z)$ and $q(z)$ have suitable behavior during the early to current times and can cover the current acceleration, our study shows that proper behavior is not obtainable for $z < 0$.

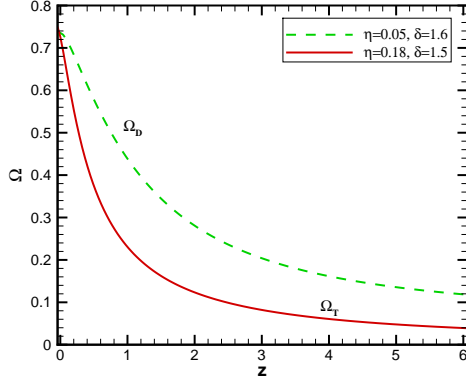


FIG. 13: The Ω_T and Ω_D against z for the non-interacting THDE model for the common (solid line) and new (dash line) approach in Rastall theory.

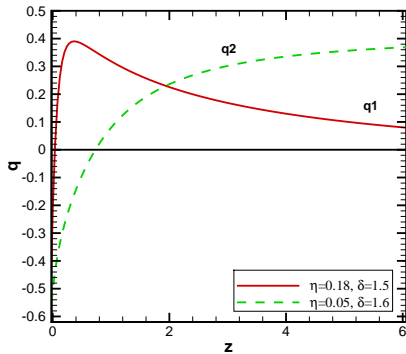
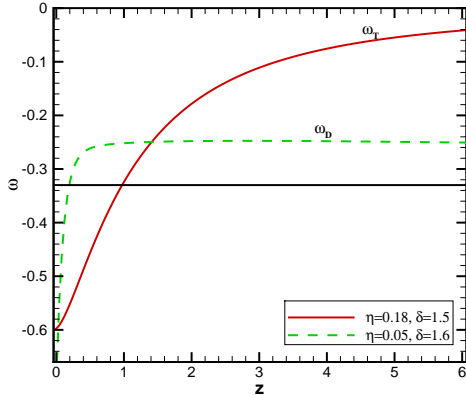


FIG. 14: The ω and q against z for the non-interacting THDE model for the common (solid line) and new (dash line) approach in Rastall theory.

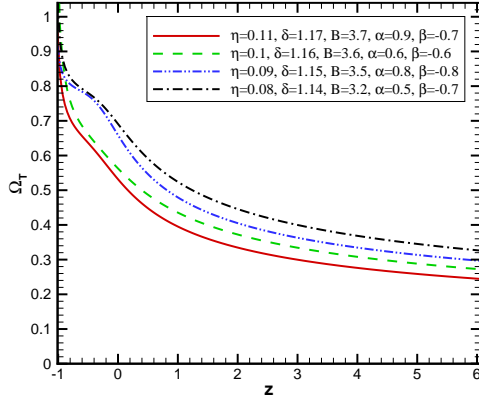


FIG. 15: Ω_T against z for the interacting THDE model in Rastall theory. We have taken $\Omega_T(z = 0) = 0.73$ as the initial condition.

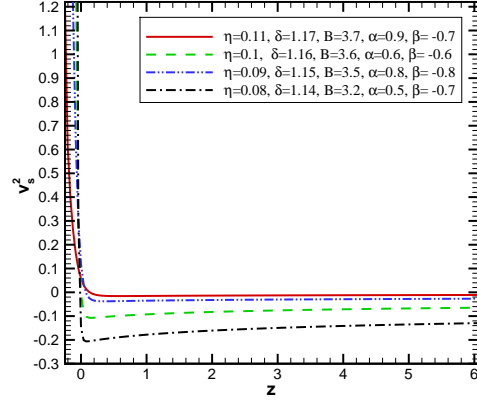


FIG. 17: v_s^2 against z for the interacting THDE model in Rastall theory.

An interacting case

For interacting case, by using Eqs. (8), (14), (21), (38) and (40), we can find

$$\begin{aligned} \Omega'_\eta = & \frac{4\eta - 1}{(1 - 6\eta)(3\eta - 1)} \left[(\alpha - 3)(1 - 6\eta)\Omega_\eta \right. \\ & + (4\eta - 1) \left((\alpha - 3)(1 - \Omega_T - 6\eta) + \beta\Omega_T \right) \\ & \left. + \frac{(3\eta - 1)\Omega_\eta}{\eta} ((2 - \delta)\Omega_T + 6\eta - 1) \right] - \frac{\Omega_\eta^2}{\eta}. \end{aligned} \quad (44)$$

The behavior of the dimensionless density parameter, EoS and deceleration parameters for interacting THDE in Rastall theory are plotted in Figs. 15 and 16. Figure 15 shows that $\Omega_T \rightarrow 0$ at the early time and $\Omega_T \rightarrow 1$ at future ($z \rightarrow -1$), as a desired result. It is also obvious that Universe has a transition from the deceleration phase to the current accelerated phase at the redshift $z \approx 0.6$, and unlike the non-interacting case, the interacting THDE model can produce acceptable behavior at future, and its EoS parameter can cross the phantom line.

Combining the time derivative of Eq. (41) with Eqs. (38), (40) (44) and (17), one can also obtain v_s^2 for interacting THDE in the Rastall theory. Since this expression is too long, we shall not present it here, and only a plot of it in Fig. 17 is presented, showing that the THDE model in Rastall theory is classically stable.

B. The second approach

In this case, using $\rho_c = \frac{3H^2(6\eta-1)}{\kappa_G(4\eta-1)}$ in rewriting the dimensionless density parameters of THDE as

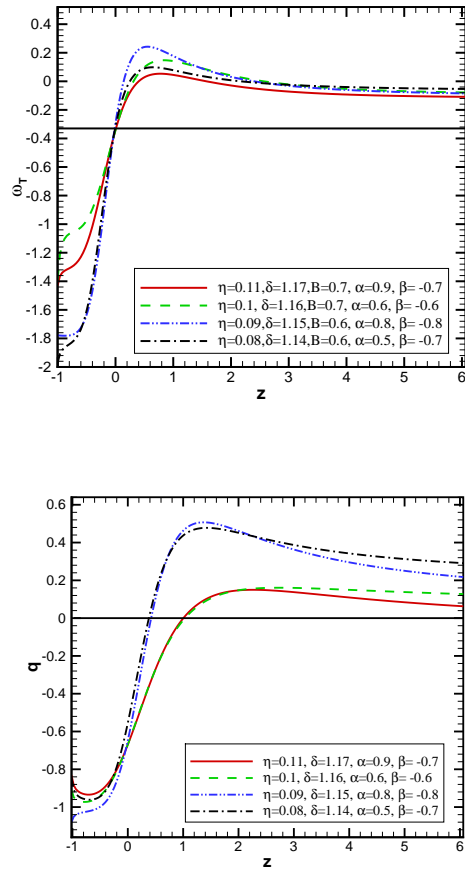


FIG. 16: ω_D and q against z for the interacting THDE model in Rastall theory.

$$\Omega_T = BH^{2-2\delta}, \quad (45)$$

where B is a known parameter as usual [12], and using Eq. (28) leading to

$$\Omega_D = \Omega_T + 4\eta + 2\eta \frac{\dot{H}}{H^2}, \quad (46)$$

and combining it with Eq. (45), one reaches at

$$\Omega'_T = \frac{(1-\delta)(\Omega_D - \Omega_T - 4\eta)\Omega_T}{\eta}. \quad (47)$$

Calculations for the EoS parameter and q also yield

$$\omega_D = \frac{-1}{3\eta\Omega_D} (\Omega_D - \Omega_T - \eta), \quad (48)$$

and

$$q = \frac{-1}{2\eta} (\Omega_D - \Omega_T - 2\eta), \quad (49)$$

respectively. It is finally useful to mention here that Eqs. (47)–(48) and (49) are valid for both interacting and non-interacting cases.

Non-interacting Case

Taking the derivative with respect to time from Eq. (25) and using Eqs. (10), (38), (46) and (27), we reach at

$$\begin{aligned} \frac{\ddot{H}}{H^3} &= \frac{3(4\eta - 1)(\Omega_D - 1)}{2\eta(1 - 3\eta)} \\ &- \frac{1}{2\eta^2} ((2 - \delta)\Omega_T + 4\eta - 1)(\Omega_D - \Omega_T - 4\eta). \end{aligned} \quad (50)$$

Now by taking the time derivative of Eq. (46) and using Eqs. (47) and (33), one finds

$$\Omega'_D = (\Omega_D - 1) \left(\frac{3(4\eta - 1)}{1 - 3\eta} - \frac{\Omega_D - \Omega_T - 4\eta}{\eta} \right). \quad (51)$$

We have also plotted the behavior of $\Omega_D(z)$, $\omega_D(z)$ and $q(z)$ in Figs. 13 and 14 which show that, even in the second approach, the non-interacting THDE model can not still produce suitable behavior at future ($z < 0$).

An interacting Case

The evolution of Ω_D , by combining Eqs. (21), (38), (46) and (27) with the time derivative of the first Friedmann equation (25), is obtained as

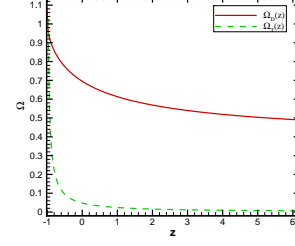


FIG. 18: Ω_D and Ω_T versus z for interacting THDE for the second approach, where the different parameters $\Omega_D(z=0) = 0.73$, $\eta = 0.96$, $\delta = 1.3$, $\alpha = 0.71$ and $\beta = -0.23$ are adopted.

$$\begin{aligned} \Omega'_D &= \frac{4\eta - 1}{1 - 3\eta} ((\alpha - 3)(1 - \Omega_D) + \beta\Omega_T) \\ &- \frac{1}{\eta} (\Omega_D - 1)(\Omega_D - \Omega_T - 4\eta). \end{aligned} \quad (52)$$

ω_D and Ω_T as the functions of redshift have been plotted in Fig. 18 indicating that $\Omega_D \rightarrow 1$ and $\Omega_T \rightarrow 1$ in future and we have $\Omega_T \rightarrow 0$ and $0.1 \lesssim \Omega_D < 0.3$ in the past. Indeed, while the Rastall term have more contribution in Ω_D in the past, the portion of vacuum energy (Ω_T) is increased by decreasing z and will get dominant at future. In Fig. 18, the behavior of $\omega_D(z)$ and $q(z)$ are also plotted. Taking the time derivative of relation (48) and considering Eqs. (17) and (51), one can obtain v_s^2 for interacting THDE model in the second approach. Since this expression is too long, we have only plotted it in Fig. 20 rather than presenting it.

IV. COMPARISON OF THE THEORETICAL MODELS WITH THE OBSERVATIONAL HUBBLE PARAMETER DATA

In Figs. 21-24, we have shown the evolution of normalized Hubble parameter $h(z) = \frac{H(z)}{H_0}$ for our models and compared it with that of the data points for normalized Hubble parameter with 1σ error bars which have been obtained from the compilation of 41 points of $H(z)$ measurements [29, 30] using the present value of $H(z)$ from [31]. The corresponding error in $h(z)$ is given as [32]

$$\sigma_h = h \sqrt{\frac{\sigma_{H_0}^2}{H_0^2} + \frac{\sigma_H^2}{H^2}} \quad (53)$$

where, σ_H^2 , $\sigma_{H_0}^2$ are errors in H and H_0 respectively.

We found that for most of the cases, our models quite fit well with the latest $H(z)$ dataset at low redshifts. Furthermore, we also checked that the nature of the evolution of $h(z)$ is hardly affected by a small change in the

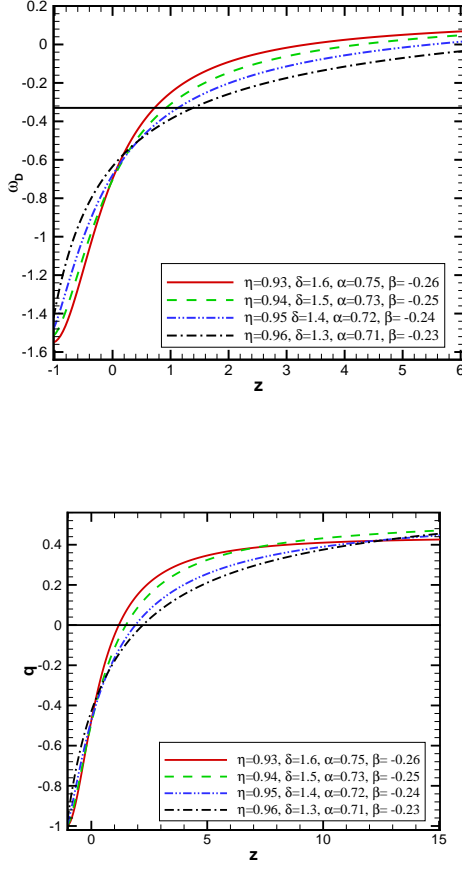


FIG. 19: The evolution of the equation of state ω_D and deceleration parameters q with respect to the redshift z for the interacting THDE for the second approach.

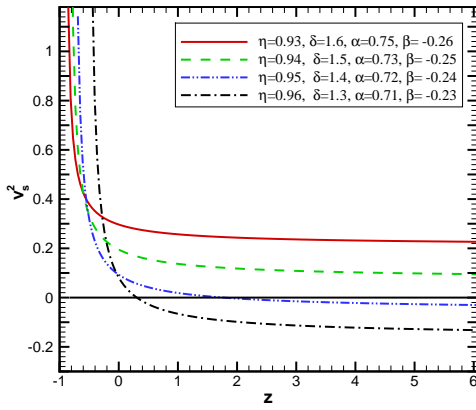


FIG. 20: v_s^2 and Ω_T versus z for interacting THDE model for the second approach.

values of the model parameters. Therefore, we conclude that our models are consistent with the $H(z)$ data in the comfortable region of the parameter space.

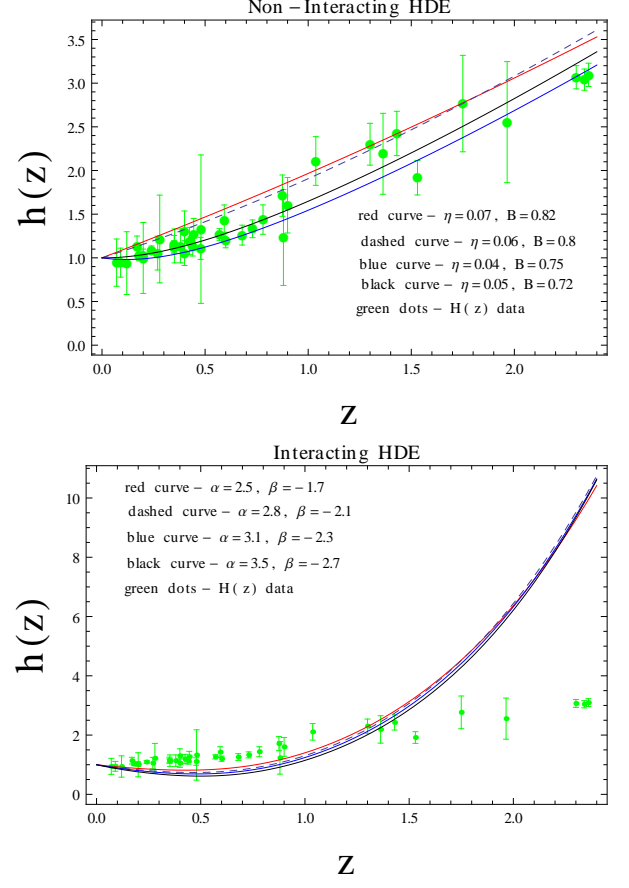


FIG. 21: The evolutions of the normalized Hubble parameter is shown with respect to the redshift z for the non-interacting HDE model (upper panel) and the interacting HDE model (lower panel) with common approach in Rastall theory. The lower panel is for $\eta = 0.11$ and $B = 1.2$. The green dots correspond to the normalized Hubble parameter data consisting 41 data points [29, 30] with 1σ error bars.

V. SUMMARY

We found out that, the same as the original HDE in standard cosmology [9], the density dimensionless parameter of HDE in Rastall framework is constant in common approach. The behavior of deceleration and EoS parameters is suitable in both interacting and non-interacting regimes. In the second approach, while the sum of HDE and Rastall parameter plays the role of dark energy, unlike the common approach, the density dimensionless parameter is not constant during the cosmic evolution. In this manner and in the presence of interaction, all cosmological parameters show acceptable behavior with the

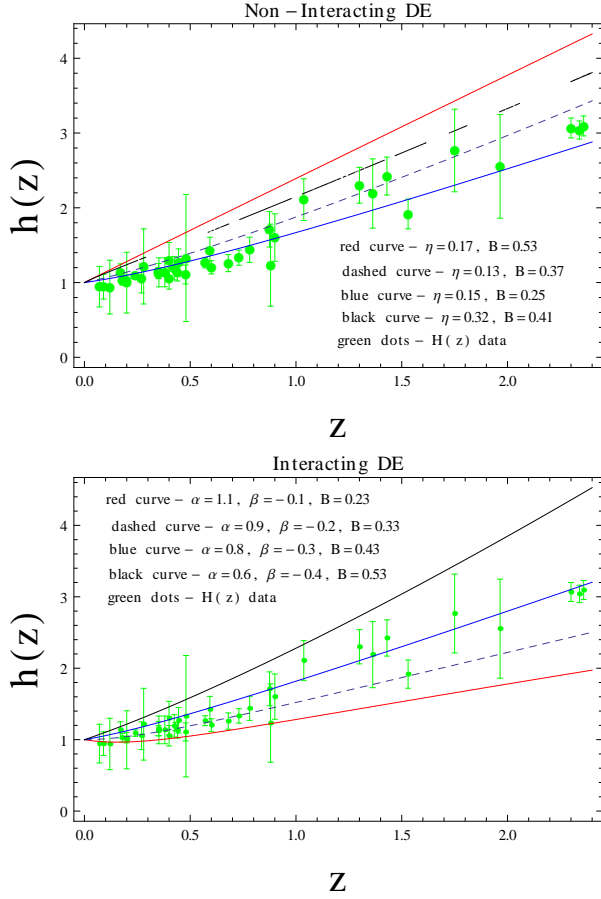


FIG. 22: The evolutions of the normalized Hubble parameter is shown with respect to the redshift z for the non-interacting DE model (upper panel) and the interacting DE model (lower panel) with new approach in Rastall theory. The lower panel is for $\eta = 0.1$.

same values of the coupling constants including η , α and β , an outcome which may not be obtained in the absence of the assumed mutual interaction between vacuum energy and dark matter.

Our study implies the fact that the density dimensionless parameter of THDE (Ω_T) is not always constant during the cosmic evolution, and the cosmic parameters show proper behavior by themselves only whenever the mutual interaction is present between the vacuum energy and dark matter. The same conclusion is also valid in the second approach. It is finally useful to mention that only the non-interacting HDE in common approach is always classically unstable. We also found that the models are consistent with the latest $H(z)$ data at low redshifts for a wide range of the values for the models parameters.

-
- [1] H. Moradpour, *Int. Jour. Theor. Phys.* **55**, 4176 (2016).
[2] R. C. Nunes et al., *JCAP* 08, 051 (2016).
[3] N. Komatsu, *Eur. Phys. J. C* **77**, 229 (2017).
[4] H. Moradpour et al., *Phys. Rev. D* **96**, 123504 (2017).
[5] A. G. Cohen, D. B. Kaplan, A. E. Nelson, *Phys. Rev. Lett.* **82**, 4971 (1999).
[6] P. Horava, D. Minic, *Phys. Rev. Lett.* **85**, 1610 (2000).
[7] S. Thomas, *Phys. Rev. Lett.* **89**, 081301 (2002).
[8] S. D. H. Hsu, *Phys. Lett. B* **594**, 13 (2004).
[9] M. Li, *Phys. Lett. B* **603**, 1 (2004).
[10] Y. S. Myung, *Phys. Lett. B* **652**, 223 (2007).
[11] L. P. Chimento, M. I. Forte, M. G. Richarte, *Mod. Phys. Lett. A* **28** (2013) 1250235; L. P. Chimento, M. I. Forte, M. G. Richarte, *The European Physical Journal C* **73**, 2285 (2013); L. P. Chimento and M. G. Richarte, *Phys. Rev. D* **84**, 123507 (2011).
[12] M. Tavayef et al., *Phys. Lett. B* **781**, 195 (2018). more12 V. C. Dubey et al., *Int. J. Geom. Method. Mod. Phys.* DOI: 10.1142/S0219887820500115 (2019).
[13] T. Josset, A. Perez, *Phys. Rev. Lett.* **118**, 021102 (2017).
[14] H. Moradpour et al., *AHEP* 7124730 (2018).
[15] F. Darabi et al., *Eur. Phys. J. C* **78**, 25 (2018).
[16] P. Rastall, *Phys. Rev. D* **6**, 3357 (1972).
[17] H. Moradpour, I. G. Salako, *AHEP*, 3492796 (2016).
[18] F. F. Yuan, P. Huang, *Class. Quantum Grav.* **34**, 077001 (2017).
[19] R. Li et al., *MNRAS*. **486**, 2407 (2019).
[20] T. Manna, F. Rahaman, M. Mondal, *Mod. Phys. Lett. A* 2050034 (2019). DOI: 10.1142/S0217732320500340.
[21] M. Capone, V. F. Cardone and M. L. Ruggiero, *J. Phys. Conf. Ser.* **222**, 012012 (2010).
[22] C. E. M. Batista et al., *Phys. Rev. D* **85**, 084008 (2012).
[23] Akarsu Ö. et al., arXiv:2004.04074v1.
[24] M. Roos, *Introduction to Cosmology* (John Wiley and Sons, UK, 2003).
[25] D. Pavon and W. Zimdahl, *Phys. Lett. B* **628**, 206 (2005).
[26] R. A. Daly et al., *Astrophys. J.* **677**, 1 (2008); E. Komatsu et al. [WMAP Collaboration], *Astrophys. J. Suppl.* **192**, 18 (2011).
[27] O. Bertolami, F. Gil Pedro, M. Le Delliou, *Phys. Lett. B*

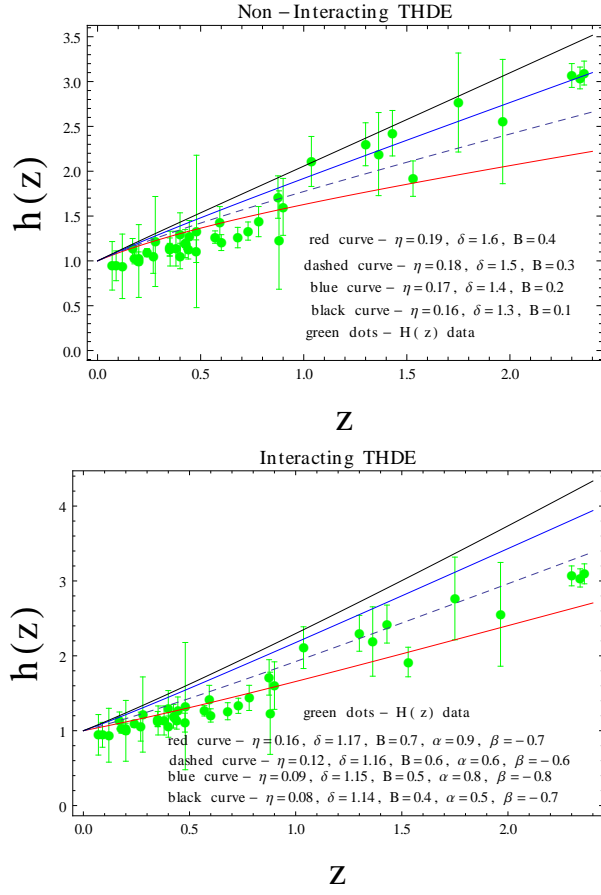


FIG. 23: The evolutions of the normalized Hubble parameter is shown with respect to the redshift z for the non-interacting THDE model (upper panel) and the interacting THDE model (lower panel) with common approach in Rastall theory.

- 654 (2007) 165;
O. Bertolami, F. Gil Pedro, M. Le Delliou, Gen. Relativ. Gravit. **41** (2009) 2839.
[28] E. Abdalla et al., Phys. Lett. B 673 (2009) 107;
B. Wang, E. Abdalla, F. Atrio-Barandela and D. Pavon, Rep. Prog. Phys. **79** (2016) 096901
[29] X.-L. Meng et al., arXiv:1507.02517 (2015).
[30] M. Moresco et al., JCAP, **05**, 014 (2016).
[31] A. G. Riess et al., ApJ, **826**, 56 (2016).
[32] A. A. Mamon, S. Das, Int. J. Mod. Phys. D., **25**, 1650032 (2016).

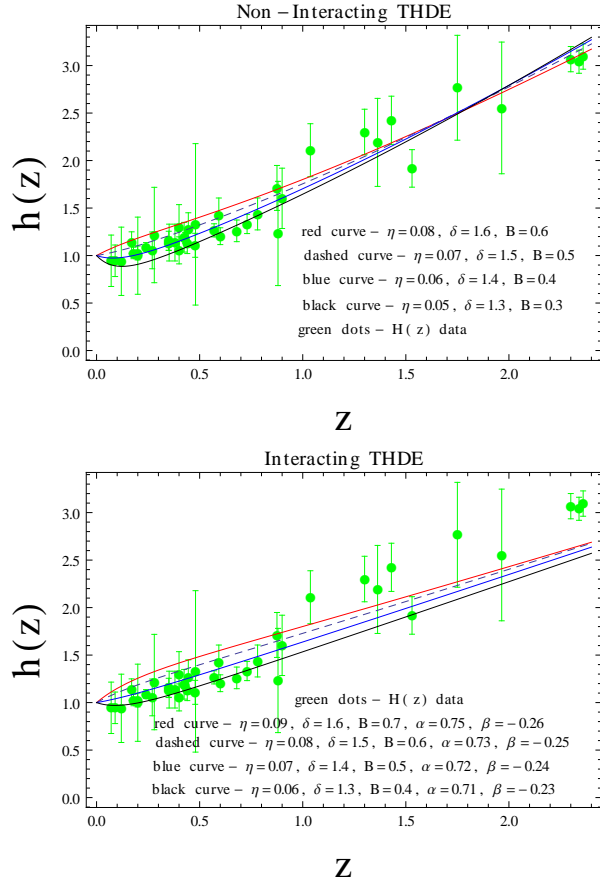


FIG. 24: The evolutions of the normalized Hubble parameter is shown with respect to the redshift z for the non-interacting THDE model (upper panel) and the interacting THDE model (lower panel) with new approach in Rastall theory.

This figure "OmegaDT22.jpg" is available in "jpg" format from:

<http://arxiv.org/ps/2002.04972v4>